lubricants

MDPI

Article

Experimental Verification and Multi-Physics-Based Computer-Aided Engineering Simulation Methods for Dynamic Characteristics Analysis of Gas Foil Bearings at Lift-Off State

Tai-Yuan Yu * and Pei-Jen Wang

The Department of Power Mechanical Engineering, National Tsing Hua University, No. 101, Sec. 2, Guangfu Rd., East Dist., Hsinchu City 30013, Taiwan; pjwang@pme.nthu.edu.tw

* Correspondence: www6112000@gmail.com

Abstract: This paper presents an analysis of the dynamic characteristics observed and studied during the startup process of a gas foil radial bearing. It utilizes a comparison of both experimental data and three-dimensional fluid–solid interaction computational fluid dynamics simulations to investigate a gas foil bearing with three bump-type pads. The analytical model employs the fluid–structure interaction finite element method to examine the relationship between the components and the thin working fluid film within the bearing. This analysis was conducted under various operational conditions, including ambient pressure and temperature, shaft rotational speed, and the load applied to the shaft within the bearing. The foil structure of the bearing was modeled by representing the top and bump foils as a series of linear springs that are interconnected with the rigid housing. Meanwhile, the hydrodynamic pressure distribution acting on the top foil was modeled as a gas film operating under steady-state lubrication conditions. The comprehensive three-dimensional multi-physics model was developed using a commercial computer-aided engineering package, enabling independent finite element calculations for both fluid and solid domains. Following these calculations, the model exchanged analysis results across the interface between domains, allowing simulations to continue until the system achieved a quasi-steady state. An in-house experimental system was designed to evaluate the performance of the gas foil bearing under different working conditions, including the load applied to the shaft and the rotational speed. The experiment investigated the operational state of a gas foil radial bearing under ambient pressure (1 bar), ambient temperature (303 K), rotational speeds ranging from 1.5 to 9.5 krpm, and a load of 0.5602 kgw. Some operational conditions of the bearing were defined as boundary condition inputs for the simulation model. The model's results, notably the predicted lift-off rotational speed of the bearing, show strong alignment with results from in-house experiments.

Keywords: computational fluid dynamics; fluid–structure interaction multi-physics simulations; lift-off rotational speed of gas foil bearing

check for updates

Received: 16 January 2025
Revised: 6 February 2025
Accepted: 8 February 2025
Published: 10 February 2025

Citation: Yu, T.-Y.; Wang, P.-J. Experimental Verification and Multi-Physics-Based Computer-Aided Engineering Simulation Methods for Dynamic Characteristics Analysis of Gas Foil Bearings at Lift-Off State. *Lubricants* **2025**, *13*, 75. https://doi.org/10.3390/lubricants13020075

Copyright: © 2025 by the authors. Licensee MDPI, Basel, Switzerland. This article is an open access article distributed under the terms and conditions of the Creative Commons Attribution (CC BY) license (https://creativecommons.org/licenses/by/4.0/).

1. Introduction

In the early years of this century, gas foil bearings (GFBs) were successfully implemented in micro turbomachinery, including generators, turbochargers, and compressors [1]. GFBs provide high operational efficiency by stabilizing the shaft during high-speed operation, as their friction forces are significantly lower than those of traditional bearings are. Furthermore, they directly utilize the surrounding working fluid as a lubricant. As a result, systems equipped with this type of bearing require neither sealing nor the use of oil-based

lubricants. These attributes position GFBs as a highly promising bearing technology for applications demanding high rotational speeds, compact design, and superior efficiency. The primary characteristic of GFBs is their compliant foil structure, which provides load capacity, operational stiffness, and damping effects during shaft rotation. In GFBs, the top and bump foils, together referred to as the foil structure, function as compliant components. The rotating shaft generates shear stress within the thin fluid film between the top foil and shaft surface, driving the working fluid through this gap. Consequently, hydrodynamic pressure generates a supporting force to stabilize the shaft. Variations in the foil structure configuration influence a bearing's dynamic performance, impacting parameters like pressure and temperature distribution within the thin film, as well as stiffness and damping coefficients under specific operating conditions. Figure 1 presents a photo representation and highlights the main components of typical bump-type GFBs manufactured by researchers.

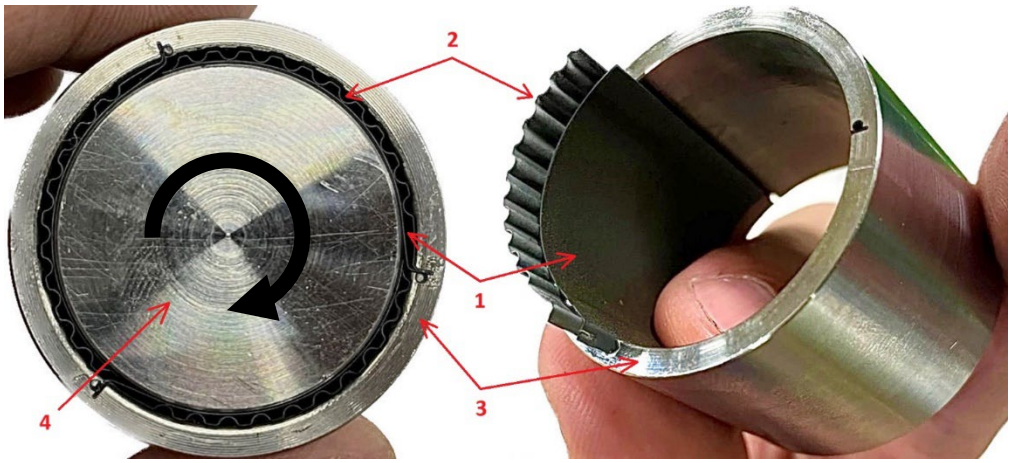


Figure 1. Photo of bump-type GFBs. The main parts of GFBs include 1. the top foil, 2. the bump foil, 3. the housing, and 4. the shaft. The clockwise arrow indicates the shaft's rotational direction.

In recent years, the growing importance of GFBs in turbomachinery applications has led to a significant increase in research across multiple disciplines, resulting in numerous reported findings. In the late 20th century, Ku and Heshmat developed a theoretical model to analyze the performance of GFBs featuring a deformable and compliant structure [2]. This analytical model incorporated the interaction forces among bearing parts during shaft rotation within it, including load, friction force, and shear stress in the working fluid film. Subsequently, Dellacorte and Valco introduced design guidelines to aid researchers in implementing GFBs within turbomachinery applications [3]. Their research revealed that the load capacity of GFBs increases in proportion to the rotational speed of the shaft. Additionally, their study examined the impact of various design factors on load capacity, including size and bearing configuration. Peng and Carpino conducted an analysis of a bearing's damping coefficient and dynamic stiffness under different shaft rotational speeds, utilizing an ideal gas assumption [4]. Peng and Khonsari conducted an analysis of the thermo–hydrodynamic behavior of a GFB with a 50 mm shaft diameter, testing operational speeds between 10 and 30 krpm, and confirmed their results through experimental validation [5]. Their findings suggest that assuming non-isothermal gas conditions results in reduced load capacity. San Andrés and Kim provided predictions for the deformation of the top foil and gas pressure distribution using finite element methods (FEMs) to analyze bearing performance at operating speeds of 30,000 and 45,000 rpm [6]. Carpino and Talmage developed a fluid–structure interaction (FSI) simulation model using FEMs to estimate the arrangement patterns of pressure and temperature fields, as well as the shaft

position, during bearing operation [7,8]. Following that, Song and Kim introduced a new elastic foil structure for assembling GFBs, with its performance characteristics validated through experimentation [9]. Their model incorporates shaft vibration behavior to forecast the operational features of GFBs. Furthermore, Kim examined the performance differences between single and three-pads-type GFBs [10]. Their study concluded that the geometry and layout of a bearing impact the working characteristic behavior of the shaft more significantly than the stiffness of the foil structure. Le Lez et al. proposed both dynamic and static models to investigate the operating property of the foil structure in GFBs, presenting an analytical model that treats the foil structure as an independent spring for predicting dynamic features [11–14]. They applied this model to simulate the imbalance response of GFBs, validating their results through experimental results. Regarding the thermal boundary conditions in GFBs, Dykas and Howard examined the heat transfer phenomena under light loading conditions, concluding that the primary factor influencing thermal behavior is the bearing configuration [15]. Heshmat and colleagues investigated the diverse applications of GFBs in high-temperature environments, including uses in turbojet engines [16–20]. Kim and Park addressed challenges associated with initial sliding contact by introducing hybrid gas foil bearings that incorporate a hydrostatic design, providing a hydrostatic lift feature [21]. This innovative approach offers several advantages over traditional GFBs. First, it reduces the torque required to initiate operation. Second, it enhances a bearing's load capacity, allowing it to support greater loads effectively.

Zhou, Yu et al. conducted research on the thermal characteristics of bearings under various operating conditions and proposed a method to monitor, confirm, and manage a bearing's operating state based on temperature [22]. Their study encompassed a range of rotational speeds, allowing dynamic characteristics during startup and stopping stages of a bearing to be analyzed. As a result, this method also enabled the estimation of a bearing system's lifecycle.

Martowicz et al. proposed an effective sensing method capable of directly confirming the temperature distribution pattern on the top foil of a bearing [23]. This is crucial because the temperature field influences bearings, as nearly all aerodynamic and thermomechanical effects are temperature-dependent. The complete working cycle, including both startup and stopping stages, was validated through experimentation.

After that, Martowicz et al. presented a novel thermomechanical and thermal sensing method for bearings, with its usability confirmed by the results of in-house experiments [24]. Their relevant study considered several important operating conditions of bearings, including load, rotational speed, and temperature. Rotational speeds ranged from 0 to a stable operational state, encompassing the startup rotational speed as well. Therefore, the complete working process could be verified. Additionally, various phenomena influenced by the thermomechanical effects of bearings were discussed.

2. Governing Equations of GFBs

Using the Reynolds equation as the governing model, the authors analyzed the aerodynamic characteristics of the fluid film formed between the top foil surface and the shaft [25]. Under thin-film assumptions, the thickness of the film is substantially smaller than the shaft radius, allowing the circumferential curvature to be disregarded. Figure 2 provides additional details [26]. When the shaft and bearing hole axes are parallel, the Reynolds equation is represented in cylindrical coordinates as Equation (1).

$$\frac{1}{R^2}\frac{\partial}{\partial\theta}\left(\frac{\rho h^3}{\mu}\frac{\partial p}{\partial\theta}\right)+\frac{\partial}{\partial z}\left(\frac{\rho h^3}{\mu}\frac{\partial p}{\partial z}\right)=6\omega\frac{\partial(\rho h)}{\partial\theta}+12\frac{\partial(\rho h)}{\partial t} \quad (1)$$

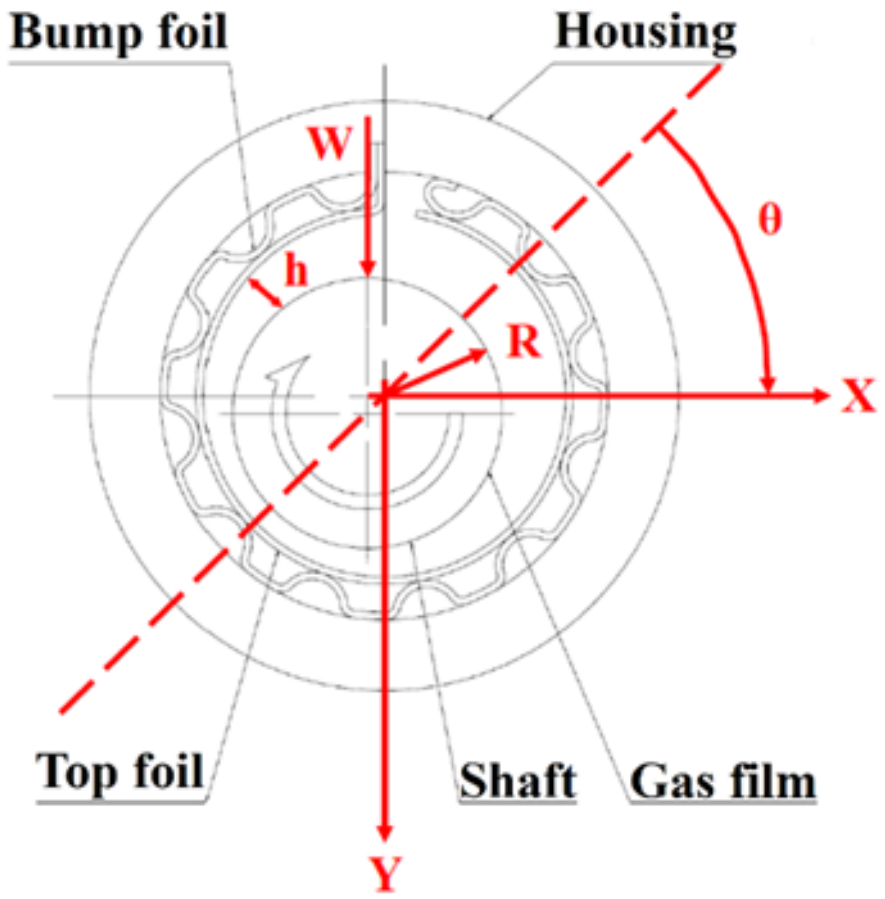


Figure 2. Schematic diagram of typical bump-type gas foil bearing [26].

3. Discussion of Experimental Methodology for Bearing Startup Resistance Force

To confirm the operational characteristics of bearings during the startup phase, an internal experimental bench was constructed to examine the relationship between a bearing's startup resistance force and the rotational speed of the shaft. Details regarding the setup method and configuration of this test bench are provided in Figure 3. A shaft with a diameter of 30 mm was driven directly by a high-speed motor, while a GFB with a nominal inner diameter of 30.05 mm was designed and fabricated by the authors. This GFB was aligned with the shaft, and the friction force resulting from the relative sliding between the top foil and the shaft surface was transmitted through a stick to a load cell, Model 9217A (Kistler, Winterthur, Switzerland), positioned 87 mm radially from the shaft center. The load cell thereby provided an accurate measure of the friction force acting on the bearing generated by the shaft during operation, particularly during the phase when the shaft reached the critical startup rotational speed. Additionally, calibration weights were used to apply load to the bearing by generating a tension force, allowing the experimental bench to simulate conditions in which load is applied from the shaft to the bearing during operation. It should also be noted that the exact inner diameter of the GFB manufactured in-house by the authors was 30.0388 mm, as measured using a bridge-type coordinate measuring machine, a Contura (ZEISS, Oberkochen, Germany).

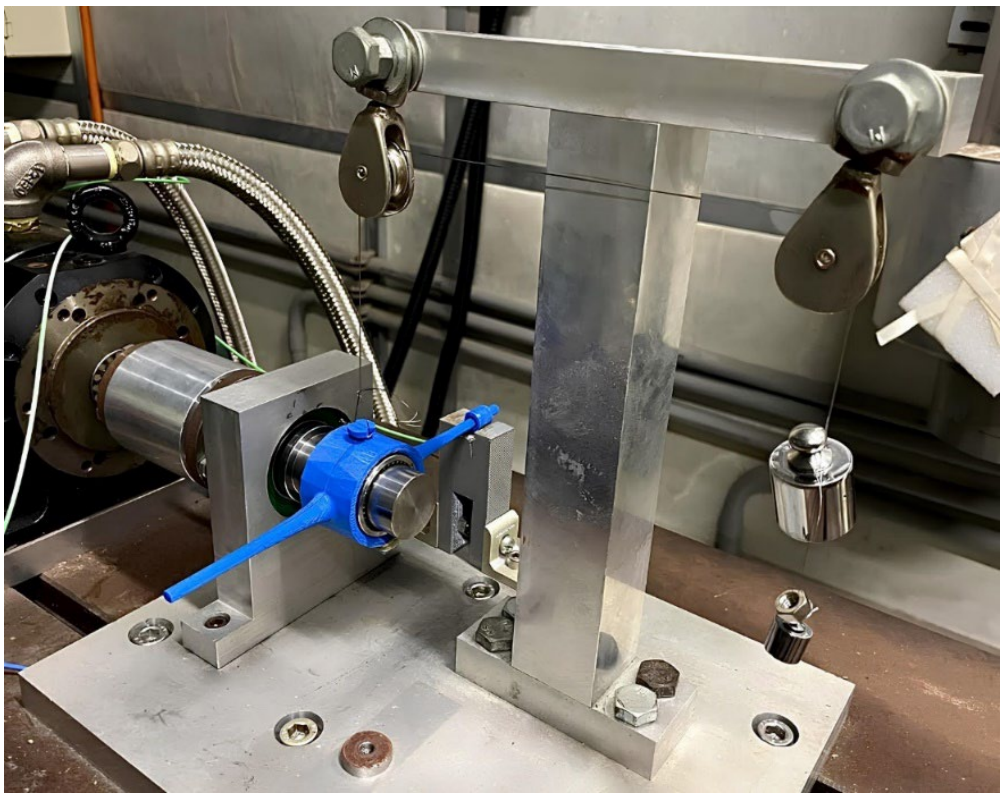


Figure 3. Photograph of the experimental bench for measuring a bearing's startup resistance force.

4. Discussion of Analysis Methodology of FSI Simulation Model near Bearing Startup Rotational Speeds

To comprehensively evaluate the operational characteristics of both fluid and solid regions, particularly near the startup rotational speed of a bearing, detailed study results were published by the authors in a previous paper. That research explored crucial aspects such as the meshing strategy, boundary condition setup, and geometry creation process of the simulation model [26]. Furthermore, a similar simulation methodology and associated settings were employed to examine gas foil thrust bearings, with findings subsequently also reported by the authors [27]. The fluid domain in the bearing corresponded to the thin gas film, while the solid domain related to the shaft. Detailed discussions on analysis factors are available in prior work that outlined a method for predicting the dynamic behavior of GFBs using a three-dimensional (3D) multi-physics model based on computational fluid dynamics (CFD) simulation software, Ansys Workbench 19.5 [26]. Findings demonstrate that the FSI CFD model effectively evaluated a bearing's operational behavior during startup by conducting multiple simulations series. Through a gradual increase in shaft rotational speed, dynamic parameters, such as startup speed, could be analyzed and confirmed.

Given the integration of multi-physics simulation capabilities within a commercially available computer-aided engineering package developed by Ansys Inc., Canonsburg, PA, US, this study employed that software to investigate the aerodynamic behavior of the working fluid film using the CFD module called "CFX". Additionally, the transient structure FEM module was utilized to perform elastic analysis of the foil structure. The simulation approach, grounded in a CFD-based lubrication model, aimed to replicate the dynamic performance of GFBs under specific design parameters. The analysis continued until the system stabilized in a quasi-steady state, achieving the intended operating characteristics of the bearing. The process flow chart of the conducted 3D FSI FEM simulation method is shown in Figure 4.

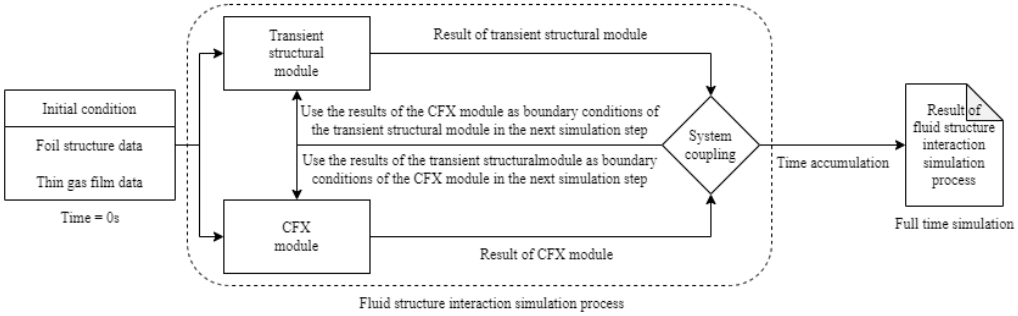


Figure 4. Process flow chart of the conducted 3D FSI FEM simulation method for GFBs [27].

In this study, the shaft mesh employed a hexahedral configuration with divisions of 36, 1, and 11 in the circumferential, radial, and axial directions, respectively. The foil structure mesh divisions were 36, 2, and 11 in the circumferential, radial, and axial directions. Table 1 provides key parameters for the GFB simulation, with environmental conditions set at 1 Bar and 30 °C. The foil structure was modeled as a homogeneous material with an equivalent stiffness of 0.1 GPa, derived from thin plate theory. Figure 5 illustrates the mesh model layout. This approach aligns with methods used in earlier bump-type foil equivalent structure analyses, as described in research by Heshmat et al. [28]. Moreover, this equivalent stiffness value was adopted in simulations performed by K. Feng and S. Kaneko to analyze GFBs [29]. The foil material used in these simulations had a Poisson's ratio of 0.3 and a Young's modulus of 214 GPa. Figure 6 presents the foil structure layout used in this study. In the simulation setup, the outer surface of the foil structure was fixed, and the shaft and bearing hole axes were maintained parallel throughout. FSI analysis began by positioning the shaft in the central region of the bearing hole. As the simulation proceeded, gravitational force caused the shaft to move downward, prompting a supportive force to develop progressively from the lower section of the bearing. This process continued until the shaft was fully supported and securely held in place. Once equilibrium was reached, the shaft achieved a quasi-steady operational state within the bearing.

Table 1. List of parameters used for 3D FSI FEM simulation model.

Parameter	Values (Unit)
Working Fluid of Gas Film	Air (ideal gas model)
Initial Pressure of Gas Film	1.0 (Bar)
Initial Temperature of Gas Film	303 (K)
Environmental Pressure	1.0 (Bar)
Environmental Temperature	303 (K)
Equivalent Stiffness of Foil Structure	0.1 (GPa)
Rotational Speed of Shaft	3, 3.5, 3.75, 4, 4.5, 5, 6 (krpm)
Surface Heat Transfer Coefficient of Foil and Shaft	100 ($W \cdot m^{-2} \cdot K^{-1}$)
Surface Temperature of Foil and Shaft	303 (K)
Load on Shaft	5.5 (N)
Mass of Shaft	0.5602 (kg)
Diameter of Shaft	30 (mm)

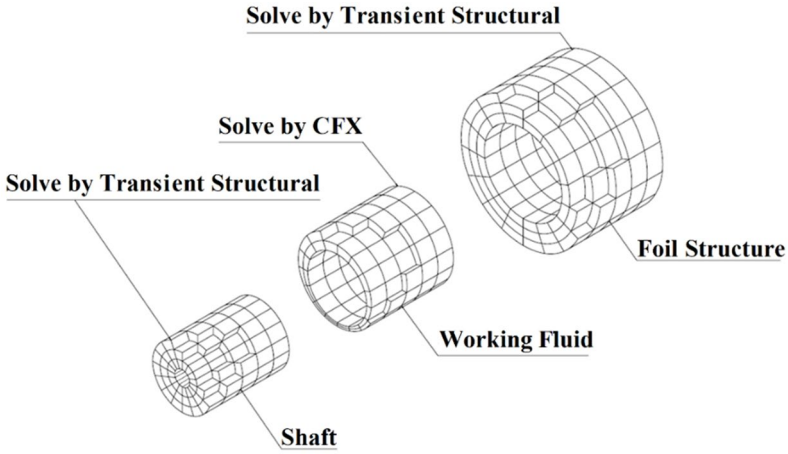


Figure 5. Three-dimensional schematic illustrations of the three interconnected physical domains used in GFB simulations within the FSI FEM model [26].

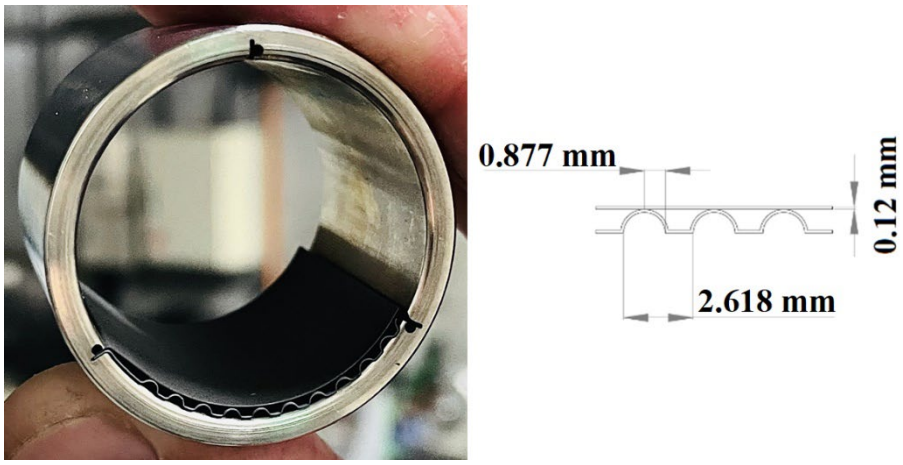


Figure 6. Schematic of the layout and measurement of the flattened foil structure of GFBs.

5. Comparison and Analysis of GFBs' Operating Characteristics at Startup Rotational Speeds

A bearing's supporting force during operation arises from the pressure differential between the upper and lower halves of the working fluid film generated by the shaft's rotation. Initially, this force is insufficient to sustain the shaft until it achieves an adequate rotational speed. Once the shaft reaches the certain speed required to produce enough force to lift it off the top foil surface and establish a thin working gas film, the shaft's inertia may cause it to lift too far from the top foil surface. Consequently, the shaft loses stability, collapsing back onto the foil surface, leading to repeated impacts and increased friction forces. This cycle persists until the shaft's rotational speed is high enough to generate sufficient damping and achieve stable operation. During this transition phase, an abrupt and irregular rise in driving torque is observed, attributed to the sudden increase in friction between the top foil surface and the shaft. These phenomena were documented not only in in-house experimental bench results, but also accurately captured in the authors' 3D FSI FEM simulation model. Please refer to Figures 7 and 8 for related information. As the rotational speed continues to increase, the working gas film grows, gradually supporting the shaft and completely lifting it off the top foil surface. At this point, the friction force reduces significantly, aligning with levels observed in unloaded bearings. Eventually, the shaft operates stably within the thin gas film, maintaining rotational motion without physical contact, exhibiting the behavior characteristics of a fully loaded bearing. Alternatively,

while three evenly distributed narrow gas supply gaps surround the bearing to create a gas film between the top foil and the shaft, this arrangement deviates slightly from the simulation model. However, when taking proportional factors and experimental findings into account, it is reasonable to assume a uniform thin gas film around the shaft during a bearing's startup phase. This assumption is justified, as friction and direct contact forces between the shaft and the top foil exert a more substantial impact on a bearing's behavior and properties than aerodynamic effects do during the startup process.

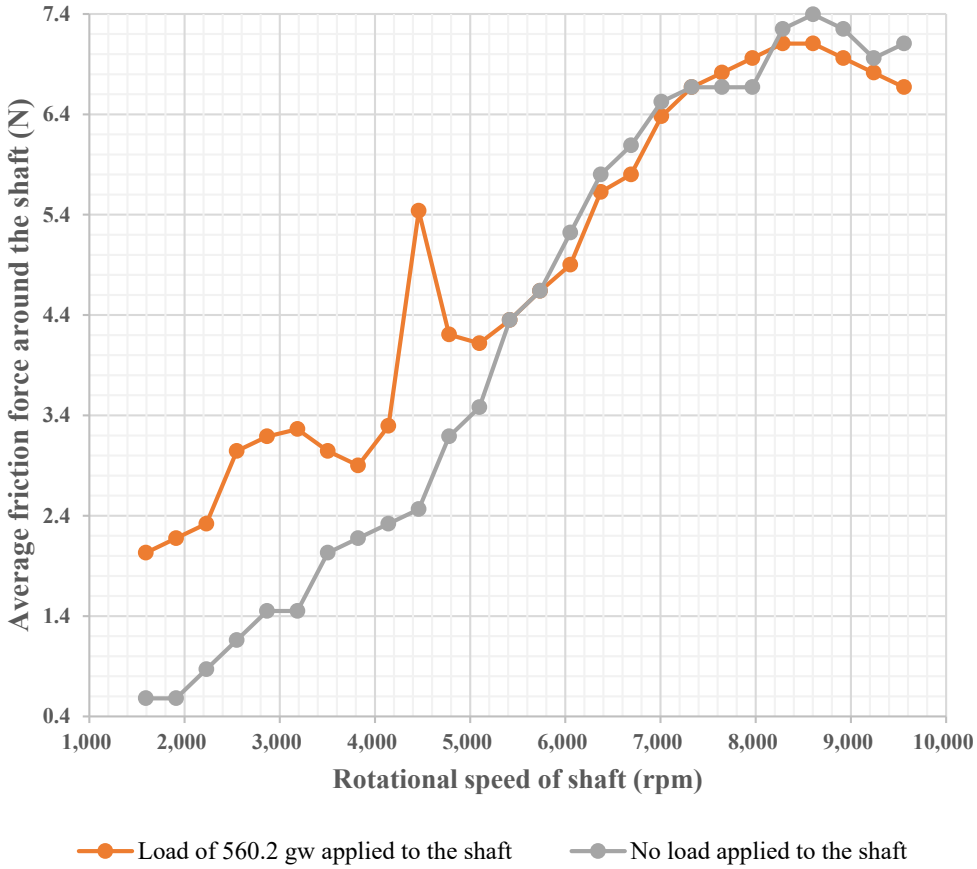


Figure 7. Composite plots showing the friction force of the 30 mm diameter shaft during its operation within GFBs with and without loading, based on results from the in-house experiment bench.

In the case discussed in this paper, when the shaft reached 4.5 krpm or higher, damped oscillation developed, indicating stable bearing operation. The proportional increase in oscillation further confirmed this. On the other hand, before reaching sufficient rotational speed, the shaft exhibited unstable vibrations to increase support, leading to a sudden torque rise at startup speed. In some cases, meshing errors caused calculation termination due to shaft-top foil collisions from insufficient support. This behavior, observable in Figure 8, particularly occurred on trajectories with rotational speeds lower than 4.5 krpm.

A series of loaded and unloaded in-house experimental results, covering approximately 1.5 to 9.5 krpm, show a sharp increase in friction force at 4.5 krpm and exhibit high uniformity with seven simulation results in the rotational speed range of 3 to 6 krpm. This consistency demonstrates the simulation model's capability to assist designers and researchers in estimating startup rotational speed during the design phase, highlighting its and usability.

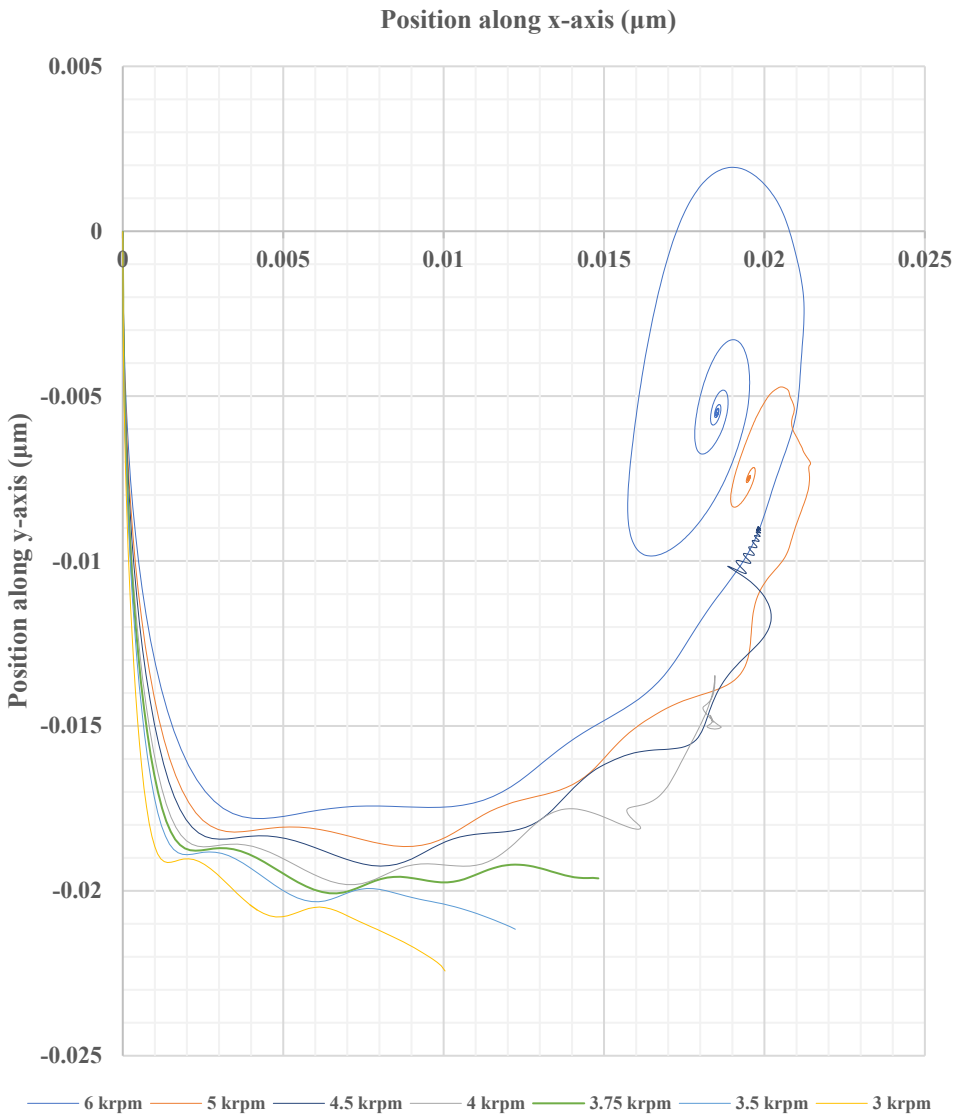


Figure 8. Composite plots illustrating the transient positions of the shaft operating within GFBs at various rotational speeds, based on the 3D FSI FEM simulation model.

For in-house experiment results, although these dynamic characteristics differ slightly from practical applications due to different bearing support methods (fixed bearings in practical applications vs. a fixed shaft on the experiment bench), a bearing's operating state could still be verified by comparing the loaded and unloaded experimental results. The frictional force on a bearing's top foil without loading was confirmed by measuring torque at various speeds using a self-weight equivalent force. These results serve as reference data for researchers. If a loaded bearing exhibits similar dynamic characteristics to an unloaded one, this indicates that the loaded bearing operates in a similar manner, with a thin, properly formed working fluid film. As the frictional force before startup is higher than it is after startup, the slight difference in the working fluid between loaded and unloaded states is negligible for usability estimates in engineering applications. This study focused on validating the estimation method based on the computer-aided engineering simulation model. The recognition of a bearing's behavior during startup, based on in-house experimental comparisons, aligned closely with the simulation model, particularly at the startup rotational speed of the gas foil bearing. Thus, experimental results validated the simulation model, demonstrating that the startup rotational speed of the bearing analyzed in this study was approximately 4.5 krpm.

6. Conclusions and Discussion

To achieve effective design and reliable management of high-speed rotational systems in industrial applications, a deep understanding of bearing behavior and precise predictive capabilities is paramount. Bearings play a critical role in ensuring smooth operation and system longevity. Among the various options available, GFBs have gained significant attention due to their unique advantages, including a non-contact operating mechanism that significantly reduces power losses and improves energy efficiency. However, despite their advantages, one major challenge lies in the instability and non-linear responses exhibited by GFBs during startup speeds, which often result in increased wear, component failure, or even complete system breakdowns. The appeal of GFBs in modern industries stems from their environmentally friendly operation, cost-effectiveness, and performance benefits. Their adoption is further supported by their compatibility with high-speed and precision applications. Nevertheless, the intricate dynamics that govern GFB operation and the experimental complexities involved in studying these bearings mean that certain behaviors—particularly during startup speeds—remain insufficiently explored and understood. This paper addresses the existing knowledge gaps by providing a detailed investigation into the startup dynamics of a GFB developed in-house. This study integrated both numerical and experimental approaches to analyze a bearing's performance. Specifically, the research employed an FSI FEM simulation model to simulate a bearing's dynamic response at startup speeds. Additionally, experimental torque measurements were conducted to validate these simulation results. Both approaches were compared, and the findings reveal a strong consistency between simulation predictions and experimental outcomes.

Although the vibration characteristics observed in the experimental and simulation models were not entirely identical, both demonstrated a clear conclusion: the bearing designed by the researcher during this study is capable of generating sufficient supporting force at rotational speeds ranging from approximately 4 to 5 krpm. Results presented in this paper not only provide a clearer understanding of the startup characteristics of GFBs, but also offer valuable insights into factors that influence their stability and reliability during operation. This comprehensive analysis is intended to serve as a reliable reference for researchers and engineers, aiding in the design, development, and optimization of GFBs. Moreover, data and methodologies described herein can contribute to improved forecasting techniques for bearing behavior, ensuring greater operational efficiency and system reliability in future applications.

Author Contributions: Conceptualization, T.-Y.Y. and P.-J.W.; methodology, T.-Y.Y. and P.-J.W.; software, T.-Y.Y.; validation, T.-Y.Y. and P.-J.W.; formal analysis, T.-Y.Y. and P.-J.W.; investigation, T.-Y.Y. and P.-J.W.; resources, T.-Y.Y. and P.-J.W.; data curation, T.-Y.Y. and P.-J.W.; writing—original draft preparation, T.-Y.Y.; writing—review and editing, T.-Y.Y.; visualization, T.-Y.Y.; supervision, P.-J.W.; project administration, P.-J.W.; funding acquisition, P.-J.W. All authors have read and agreed to the published version of the manuscript.

Funding: This research received no external funding.

Data Availability Statement: Raw data supporting the conclusions of this article will be made available by the authors on request.

Conflicts of Interest: The authors declare no conflicts of interest.

Nomenclature

The following nomenclature is used in this manuscript.

Abbreviations

3D	Three-dimensional;
CFD	Computational fluid dynamics;
FEM	Finite element method;
FSI	Fluid–structure interaction;
GFBs	Gas foil bearings;

Notation

h	Film thickness, m;
p	Aerodynamic pressure, Pa;
R	Bearing radius, m;
t	Time, s;
W	Static load, N;
X, Y	Shaft center coordinates, m;
z	Bearing axial coordinate, m;
Greek symbols:	
θ	Bearing angular coordinate, rad;
μ	Dynamic viscosity, Pa-s;
ρ	Lubricant density, kg/m^3;
ω	Rotational speed, rad/s;

References

1. Agrawal, G.L. Foil Air/Gas Bearing Technology-An Overview. In Proceedings of the ASME 1997 International Gas Turbine and Aeroengine Congress and Exhibition, Orlando, FL, USA, 2–5 June 1997.
2. Ku, C.-R.; Heshmat, H. Compliant Foil Bearing Structural Stiffness Analysis: Part I—Theoretical Model Including Strip and Variable Bump Foil Geometry. *ASME J. Tribol.* **1992**, *114*, 394–400. [CrossRef]
3. DellaCorte, C.; Valco, M.J. Load Capacity Estimation of Foil Air Journal Bearings for Oil-Free Turbo-Machinery Applications. *STLE Tribol. Trans.* **2000**, *43*, 795–801. [CrossRef]
4. Peng, J.P.; Carpino, M. Calculation of Stiffness and Damping Coefficients for Elastically Supported Gas Foil Bearings. *ASME J. Tribol.* **1993**, *115*, 20–27. [CrossRef]
5. Peng, Z.C.; Khonsari, M. A Thermohydrodynamic Analysis of Foil Journal Bearings. *ASME J. Tribol.* **2006**, *128*, 534–541. [CrossRef]
6. San Andrés, L.; Kim, T.H. *Computational Analysis of Gas Foil Bearings Integrating 1D and 2D Finite Element Models for Top Foil*; Technical Report No. TRCB&C-1-06; Turbomachinery Laboratory, Texas A&M University: College Station, TX, USA, 2006.
7. Carpino, M.; Talmage, G. A Fully Coupled Finite Element Formulation for Elastically Supported Foil Journal Bearings. *STLE Tribol. Trans.* **2003**, *46*, 560–565. [CrossRef]
8. Carpino, M.; Talmage, G. Prediction of Rotor Dynamic Coefficients in Gas Lubricated Foil Journal Bearings with Corrugated Sub-Foils. *STLE Tribol. Trans.* **2006**, *49*, 400–409. [CrossRef]
9. Song, J.; Kim, D. Foil Gas Bearing with Compression Springs: Analyses and Experiments. *ASME J. Tribol.* **2007**, *129*, 628–639. [CrossRef]
10. Kim, D. Parametric Studies on Static and Dynamic Performance of Air Foil Bearings with Different Top Foil Geometries and Bump Stiffness Distributions. *ASME J. Tribol.* **2007**, *129*, 354–364. [CrossRef]
11. Le Lez, S.; Arghir, M.; Frene, J. Static and Dynamic Characterization of a Bump-Type Foil Bearing Structure. *ASME J. Tribol.* **2007**, *129*, 75–83. [CrossRef]
12. Le Lez, S.; Arghir, M.; Frene, J. A New Bump-Type Foil Bearing Structure Analytical Model. *ASME J. Eng. Gas Turbines Power* **2007**, *129*, 1047–1057. [CrossRef]
13. Le Lez, S.; Arghir, M.; Frene, J. A New Foil Bearing Dynamic Structural Model. In Proceedings of the ASME/STLE 2007 International Joint Tribology Conference, San Diego, CA, USA, 22–24 October 2007.
14. Lee, D.H.; Kim, Y.C.; Kim, K.W. The Dynamic Performance Analysis of Foil Journal Bearings Considering Coulomb Friction: Rotating Unbalance Response. In Proceedings of the ASME/STLE 2007 International Joint Tribology Conference, San Diego, CA, USA, 22–24 October 2007.
15. Dykas, B.; Howard, S.A. Journal Design Considerations for Turbomachine Shafts Supported on Foil Air Bearings. *STLE Tribol. Trans.* **2004**, *47*, 508–516. [CrossRef]

16. Heshmat, H.; Walton, J.F., II; Tomaszewski, M.J. Demonstration of a Turbojet Engine Using an Air Foil Bearing. In Proceedings of the ASME Turbo Expo 2005: Power for Land, Sea, and Air, Reno, NV, USA, 6–9 June 2005.
17. Heshmat, H. Operation of Foil Bearings Beyond the Bending Critical Mode. *ASME J. Tribol.* **2000**, *122*, 192–198. [CrossRef]
18. Walton, J.F.; Heshmat, H. Application of Foil Bearings to Turbomachinery Including Vertical Operation. In Proceedings of the ASME 1999 International Gas Turbine and Aeroengine Congress and Exhibition, Indianapolis, IN, USA, 7–10 June 1999.
19. Heshmat, H.; Walton, J.F.; DellaCorte, C.; Valco, M.J. Oil Free Turbocharger Demonstration Paves Way to Gas Turbine Engine Applications. In Proceedings of the ASME Turbo Expo 2000: Power for Land, Sea, and Air, Munich, Germany, 8–11 May 2000.
20. Walton, J.F., II; Heshmat, H.; Tomaszewski, M.J. Testing of a Small Turbocharger/Turbojet Sized Simulator Rotor Supported on Foil Bearing. In Proceedings of the ASME Turbo Expo 2004: Power for Land, Sea, and Air, Vienna, Austria, 14–17 June 2004.
21. Kim, D.; Park, S. Hydrostatic Air Foil Bearings: Analytical and Experimental Investigations. *Tribol. Int.* **2009**, *42*, 413–425. [CrossRef]
22. Zhou, Y.; Shao, L.; Zhao, S.; Zhu, K.; Ding, S.; Du, F.; Xu, Z. An Experimental Investigation into the Thermal Characteristics of Bump Foil Journal Bearings. *Symmetry* **2022**, *14*, 878. [CrossRef]
23. Martowicz, A.; Zdziebko, P.; Roemer, J.; Żywica, G.; Bagiński, P. Thermal Characterization of a Gas Foil Bearing—A Novel Method of Experimental Identification of the Temperature Field Based on Integrated Thermocouples Measurements. *Sensors* **2022**, *22*, 5718. [CrossRef] [PubMed]
24. Martowicz, A.; Roemer, J.; Zdziebko, P.; Żywica, G.; Bagiński, P.; Andrearczyk, A. A Novel Measurement Approach to Experimentally Determine the Thermomechanical Properties of a Gas Foil Bearing Using a Specialized Sensing Foil Made of Inconel Alloy. *Materials* **2023**, *16*, 145. [CrossRef] [PubMed]
25. Constantinescu, V.N. Basic Relationships in Turbulent Lubrication and Their Extension to Include Thermal Effects. *ASME J. Lubr. Technol.* **1973**, *95*, 147–154. [CrossRef]
26. Yu, T.-Y.; Wang, P.-J. Predictions of Dynamic Property for Gas Foil Bearings Based on Multiphysics Three-dimensional Model of Computer Aided Engineering Simulations. In Proceedings of the 10th International Conference on Fluid Flow, Heat and Mass Transfer (FFHMT'23), Ottawa, ON, Canada, 7–9 June 2023; p. 138. [CrossRef]
27. Yu, T.-Y.; Wang, P.-J. Simulation and Experimental Verification of Dynamic Characteristics on Gas Foil Thrust Bearings Based on Multi-Physics Three-Dimensional Computer Aided Engineering Methods. *Lubricants* **2022**, *10*, 222. [CrossRef]
28. Heshmat, H.; Walowit, J.A.; Pinkus, O. Analysis of Gas Lubricated Compliant Thrust Bearings. *ASME J. Lubr. Technol.* **1983**, *105*, 638–646. [CrossRef]
29. Feng, K.; Kaneko, S. Analytical Model of Bump-Type Foil Bearings Using a Link-Spring Structure and a Finite-Element Shell Model. *ASME J. Tribol.* **2010**, *132*, 021706. [CrossRef]

Disclaimer/Publisher's Note: The statements, opinions and data contained in all publications are solely those of the individual author(s) and contributor(s) and not of MDPI and/or the editor(s). MDPI and/or the editor(s) disclaim responsibility for any injury to people or property resulting from any ideas, methods, instructions or products referred to in the content.